

# $^1\text{H}$ -NMR study of endothelin, sequence-specific assignment of the spectrum and a solution structure

Vladimir Saudek, Jan Hoflack and John T. Pelton

*Merrell Dow Research Institute, 16 rue d'Ankara, 67084 Strasbourg, France*

Received 4 July 1989; revised version received 14 August 1989

The solution conformation of the recently discovered bi-cyclic, 21 amino acid vasoconstrictor peptide, Endothelin I, has been examined by  $^1\text{H}$ -NMR in deuterated dimethyl sulphoxide. A full sequential assignment has been achieved. In addition, 19 long range NOEs were detected which were employed as distance constraints in molecular dynamics calculations to yield a possible solution structure for this new peptide.

Endothelin; NMR; Conformation; Molecular modeling

## 1. INTRODUCTION

Endothelin is a bi-cyclic, 21 amino acid vasoconstrictor peptide recently isolated and characterized from cultured porcine aortic endothelial cells [1]. Recent pharmacological studies have shown that endothelin exerts a wide range of biological effects, in addition to its potent vasoconstrictor activity [2–5]. Moreover, endothelin now appears to be but one (Endothelin I) in a family of endothelin-like peptides which have a similar overall structure but different amino acid sequences [6]. In view of the expanding role that the endothelins appear to play in regulation of various mammalian systems, we have examined the  $^1\text{H}$ -NMR spectral properties of Endothelin I in dimethyl sulphoxide so as to better understand the conformational features important for its interaction with membrane receptors. In this report, we present the complete sequence-specific assignment of the  $^1\text{H}$ -NMR spectrum and a possible 3D structure derived from these data using molecular modeling techniques.

## 2. MATERIALS AND METHODS

### 2.1. Peptide synthesis

Endothelin was synthesized by standard solid-phase synthetic techniques using an automated peptide synthesizer and Boc-Trp-PAM resin [7,8]. Cysteines at positions 1 and 15 were protected by

4-methylbenzyl, while the cysteines at positions 3 and 11 were protected by acetamidomethyl. The peptide was deprotected (except the Ac groups on Cys 3 and 11) and removed from the resin with the two-step 'low-high' HF method [9]. After cyclization with 0.01 M  $\text{K}_3\text{Fe}(\text{CN})_6$  at pH 8.5 [10], the mono-cyclic analog was purified by gel filtration and preparative reverse-phase HPLC. The purified  $[\text{Cys}(\text{Ac})^3,^{11}]$ Endothelin (FAB-MS  $[\text{MH}]^+ = 2635.36$ , calc. = 2635.31) was reacted with  $\text{HgOAc}$  for 1 h, the mercuric salts removed with one equivalent  $\beta$ -mercaptoethanol in 30% acetic acid, and the peptide cyclized as before. The synthetic endothelin had an identical retention time on analytical  $\text{C}_{18}$  reverse-phase HPLC as a commercial sample (NOVA Biochem, Switzerland). Amino acid analysis after acid hydrolysis gave the proper molar ratios ( $\pm 7.0\%$ ) of the constituent amino acids; FAB-MS  $[\text{MH}]^+ = 2491.00$ , calc. = 2491.06.

### 2.2. NMR spectroscopy

Endothelin was dissolved in deuterated dimethyl sulphoxide (isotopic purity 99.96%) to a concentration of approximately 3.5 mM. Experiments were performed at 500 MHz, 37°C, on a Bruker AM500 spectrometer. A standard set [11] of two-dimensional phase sensitive spectra was obtained: correlated (COSY) [12], double quantum filtered correlated (DQF-COSY) [13], relayed coherence transfer (RELAY) [14] and nuclear Overhauser enhancement (NOESY) [15]. The data-sets were recorded in 2K blocks in the second time domain and in 0.5K blocks in the first domain. A total of 32 transients with 1.5 s relaxation delay between them were acquired at each increment. Spectra were processed on a Bruker X32 processing station with UXNMR Bruker program. Gaussian and shifted sine-bell functions were applied for apodisation. After zero-filling to 4K and 2K in the second and first dimensions, the digital resolution was 2.94 Hz/point and 5.88 Hz/point, respectively. The base-line of the spectra was corrected by fitting a third degree polynomial in both dimensions. In order to minimize the spin-diffusion effects, build-up of the nuclear Overhauser enhancement (NOE) was followed in the range of 150–500 ms. The chemical shift was referenced to 3-(trimethylsilyl)propionic-2,2,3,3- $d_4$  acid. The Brookhaven databank notation is used for the amino acid atoms (e.g. HA, HB, HG, etc. stands for the  $\alpha$ -,  $\beta$ -,  $\gamma$ - etc. hydrogens).

### 2.3. Molecular modeling

SYBYL [16] and AMBER [17] programs were used for molecular mechanics/molecular dynamics calculations. Dynamics routines were

*Correspondence address:* J.T. Pelton, Merrell Dow Research Institute, Strasbourg Research Center, 16 rue d'Ankara, 67009 Strasbourg Cédex, France

*Abbreviations:* Ac, acetamidomethyl; Boc-Trp-PAM resin, *t*-butyloxycarbonyltryptophyl-4-(oxymethyl)phenylacetamidomethyl resin; FAB-MS, fast atom bombardment-mass spectroscopy

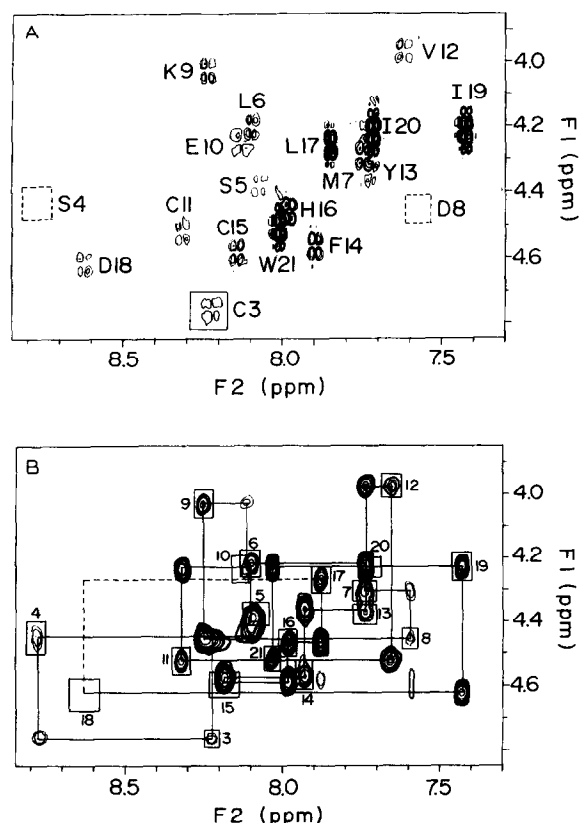


Fig.1. The fingerprint region of the spectra of endothelin showing cross-peaks between HA and HN resonances. (A) COSY spectrum. Cross-peaks of C1, S2, S4 and D8 were not detected. The position of D4 and D8 (represented by a dashed line box) were identified in the corresponding NOESY spectrum (B). C3 cross-peak (solid-line) is plotted at one contour level lower than the rest of the spectrum. (B) NOESY spectrum.  $HA_i/HN_i$  cross-peaks corresponding to the COSY peaks in A are boxed. The lines indicate the sequential connectivities by which the  $HA_i/HN_i$  and  $HA_{i+1}/HN_{i+1}$  cross-peaks are connected via a sequential cross-peak  $HA_i/HN_{i+1}$ . The dashed lines represent undetected connectivities.



















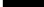



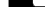


















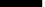







performed for 60 ps at 300 K, with conformations stored at 0.05 ps intervals. No periodic boundary conditions were applied, and the calculations were performed in the gas phase. Distance constraints for long range NOEs were entered as internal bond constraints with force constants of 20 kcal. All long range NOEs were translated to an upper limit distance of 0.5 nm to which were added the appropriate pseudo atom correction distances [11]. These values were then employed as upperbound values in the molecular dynamics calculations.

### 3. RESULTS AND DISCUSSION

A full sequential assignment was achieved using the two-stage strategy of Wüthrich [11]. A sufficient number of amino acid spin systems could be distinguished from the COSY and RELAY spectra to follow the sequence in the amide part of the spectrum. Fig.1 illustrates the sequential connectivity delineation between the  $HA_i$  and  $HA_{i+1}$ . All main-chain sequential NOEs are summarized in table 1. The sequence could

Table 1

The sequence of endothelin (SS bridges: C1–C15 and C3–C11) with a summary of the sequential connectivities

	1	5	10	15	20															
	C	C	S	S	L	M	D	K	E	C	V	Y	F	C	H	L	D	I	I	W
$\alpha/N$																				
$\beta/N$																				
N/N																				

$\alpha/N$ ,  $\beta/N$  and N/N stand respectively for  $HA_i/HN_{i+1}$ ,  $HB_i/HN_{i+1}$  and  $HN_i/HN_{i+1}$ . The symbol means that the NOE could not be detected because it was obscured by a stronger signal or that the chemical shift of the two resonances involved is nearly identical. The height of the bar indicates the intensity of the detected NOE

be followed almost entirely via  $HA_i/HN_{i+1}$ ,  $HB_i/HN_{i+1}$  and partly via  $HN_i/HN_{i+1}$  cross peaks. The analysis of the spectra thus allowed us to gain full sequential assignment of all  $^1H$ -NMR resonances detected (table 2). All aliphatic and aromatic hydrogens and all but two amide hydrogens (first two in the sequence) gave a detectable NMR signal.

Despite the low molecular mass of endothelin (~2500 Da), a large number of NOEs were recorded which were all negative. In addition to sequential NOEs, 19 long range NOEs were also detected (table 3). Furthermore, a significant spread in the chemical shifts

Table 2

$^1H$ -NMR assignments of endothelin in dimethylsulfoxide

Sequence residue		Resonances			
		HN	HA	HB	Others
No.					
1	C		3.75	2.87	3.01
2	S		4.46	3.63	
3	C	8.23	4.77	2.87	3.18
4	S	8.78	4.42	3.62	3.72
5	S	8.09	4.36	3.64	3.83
6	L	8.10	4.21	4.58	1.65HG 0.84, 0.89HD
7	M	7.44	4.30	1.87	2.04 2.42, 2.52HG 2.07HD
8	D	7.52	4.42	2.60	2.81
9	K	8.55	4.03	1.61	1.79 1.4HG 1.53HD 2.78HE
10	E	8.17	4.23	1.89	2.27 2.38HG
11	C	8.33	4.53	2.93	3.10
12	V	7.73	3.97	1.94	0.74, 0.76HG
13	Y	7.63	4.32	2.66	2.79 6.93HD 6.59HE
14	F	7.90	4.57	2.88	3.12 7.23HD 7.17HE + HZ
15	C	8.13	4.58	2.98	3.12
16	H	7.98	4.47	2.93	3.12 7.58HE1 6.84HD2
17	L	7.87	4.26	4.56	1.55HG 0.81, 0.84HD
18	D	8.62	4.62	2.50	2.78
19	I	7.43	4.22	1.69	1.38HG1 1.02HG2 0.75HD
20	I	7.70	4.21	1.72	1.41HG1 1.07HG2 0.8HD
21	W	8.02	3.05	3.15	10.76HD1 7.13HD1 7.25HE3 5.98HZ3 7.06HH3 7.33HZ2

Table 3

Summary of NOEs detected between sequentially remote residues of endothelin

Residue	Resonance	Residue	Resonance
Cys <sup>1</sup>	HA	Cys <sup>15</sup>	HA
Cys <sup>1</sup>	HA	Cys <sup>15</sup>	HB
Ser <sup>2</sup>	HA	Cys <sup>11</sup>	HB
Cys <sup>3</sup>	HA	Cys <sup>11</sup>	HB
Cys <sup>3</sup>	HA	Ser <sup>5</sup>	HA
Ser <sup>5</sup>	HA	Cys <sup>11</sup>	HB
Ser <sup>5</sup>	HB	Val <sup>12</sup>	HG
Lys <sup>9</sup>	HA	Val <sup>12</sup>	HG
Val <sup>12</sup>	HA	Cys <sup>15</sup>	HB
Val <sup>12</sup>	HG	Trp <sup>21</sup>	HB
Val <sup>12</sup>	HB	Phe <sup>14</sup>	HD
Tyr <sup>13</sup>	HD (ortho)	Phe <sup>14</sup>	HD
Phe <sup>14</sup>	HD	Val <sup>12</sup>	HB
Phe <sup>14</sup>	HD	Leu <sup>17</sup>	HD
Phe <sup>14</sup>	HD	Ile <sup>19</sup>	HG2 (CH <sub>2</sub> )
Phe <sup>14</sup>	HD	Ile <sup>20</sup>	HG2
His <sup>16</sup>	HD	Ile <sup>19</sup>	HG2
His <sup>16</sup>	HD	Ile <sup>20</sup>	HG2
Ile <sup>19</sup>	HG2	Trp <sup>21</sup>	HZ1

was observed (table 1; note for example, the very different chemical shift of all four cysteine residues). Both of these results suggest that endothelin assumes an ordered conformation in solution.

To examine the solution conformation(s) more carefully, a series of molecular energy calculations were performed. A suitable starting structure, with the C-

terminal hexapeptide in an extended random coil conformation, was generated in the following way: (i) construction of the peptide by sequentially adding amino acid building blocks; (ii) addition of the two disulfide bonds followed by energy minimization. In the molecular dynamics calculations, NMR experimental constraints were introduced. All long range NOEs (table 3) were translated to an upper limit distance of 0.5 nm with pseudo atom correction [11]. Further precision was not attempted due to uncertainty in the dependence of the mixing time (range 150–500 ms) on NOE intensity. All NOEs were, however, clearly detectable at mixing times of 300 ms or higher. Molecular dynamics calculations yield a series of very closely related compact structures in which the C-terminal hexapeptide is associated with the bi-cyclic portion of the molecule. The averaged structure for the last 400 conformations generated in the dynamics run (20 ps) was calculated and energy minimized to remove discrepancies due to averaging. The sequential NOEs, which were not employed as constraints in the molecular dynamics calculations, were now used to examine the minimized, averaged molecule. The final structure (fig.2) agrees with all the NMR data to within 0.03 nm. RMS deviations for all backbone atoms in the final 20 ps (400 conformations) are also less than 0.3 nm compared to the averaged, minimized structure.

Although considerable uncertainty in the conformations of the individual amino acid side-chains exists, the NOE data and the molecular dynamics studies define

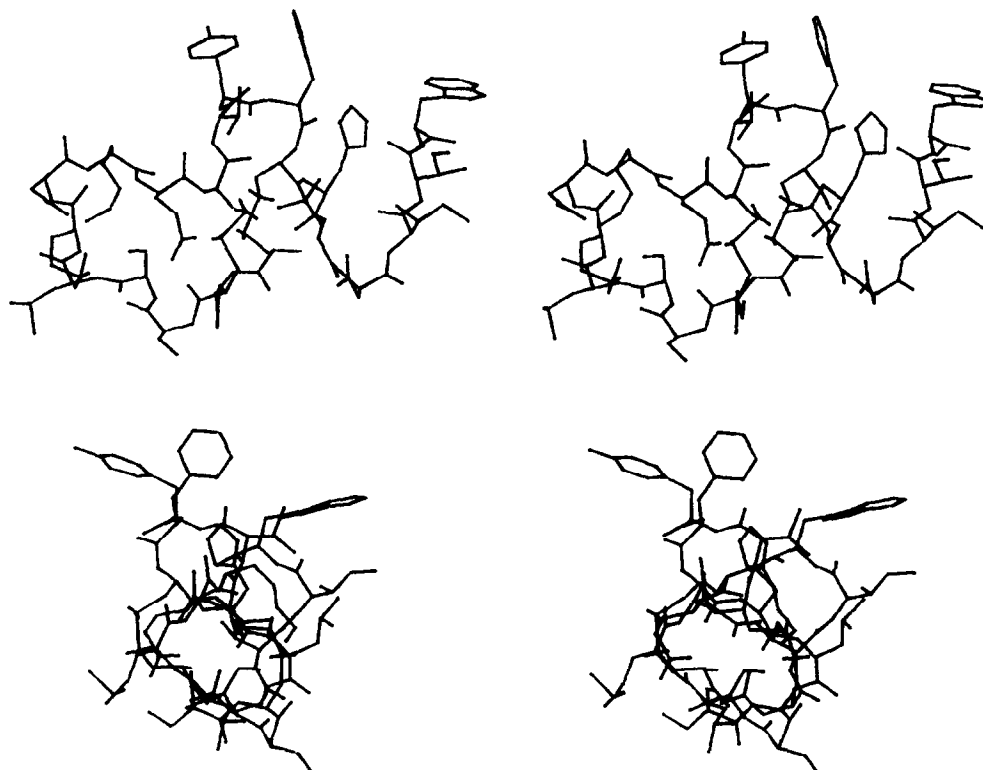


Fig.2. Stereoview of the solution conformation of Endothelin I in DMSO from NMR and molecular modeling studies.

the peptide backbone structure except for the dihedral angle of the two disulfide bonds. Assuming a standard dihedral angle of either  $\pm 90^\circ$  [18], Endothelin I may exist in any of 4 possible conformations. Molecular modeling studies indicate that the present NOE data are not sufficient to unambiguously define these two angles. Nevertheless, the structure shown in fig.2, with dihedral angles of  $-90^\circ$  (Cys<sup>1</sup>-Cys<sup>15</sup>) and  $+90^\circ$  (Cys<sup>3</sup>-Cys<sup>11</sup>), is in best agreement with our results.

#### 4. CONCLUSIONS

The <sup>1</sup>H-NMR spectrum of endothelin in deuterated DMSO has been fully assigned. The NOE spectra were utilized to provide 19 distance constraints that formed the basis for the modeling experiments and the determination of a possible solution structure (fig.2). While additional biophysical studies will be necessary to more completely define side-chain conformations, the present study shows that endothelin assumes a compact conformation in DMSO with the linear C-terminal hexapeptide closely associated with the bi-cyclic part of the molecule.

*Acknowledgements:* The authors acknowledge Dr Bernard Maigret for helpful discussions and Dr Joseph Wagner for amino acid analyses.

#### REFERENCES

- [1] Yanagisawa, M., Kurihara, H., Kimura, S., Tomobe, Y., Kobayashi, M., Mitsui, Y., Yazaki, Y., Goto, K. and Masaki, T. (1988) *Nature (Lond.)* 332, 411–415.
- [2] Fukuda, Y., Hirata, Y., Yoshimi, H., Kojima, T., Kobayashi, Y., Yanagisawa, M. and Masaki, T. (1988) *Biochem. Biophys. Res. Commun.* 155, 167–172.
- [3] Ishikawa, T., Yanagisawa, M., Kimura, S., Goto, K. and Masaki, T. (1988) *Am. J. Physiol.* 255, H970–H973.
- [4] Rakugi, H., Nakamaru, M., Saito, H., Higaki, J. and Ogihara, T. (1988) *Biochem. Biophys. Res. Commun.* 155, 1244–1247.
- [5] Uchida, Y., Ninomiya, H., Saotome, M., Nomura, A., Ohtsuka, M., Yanagisawa, M., Goto, K., Masaki, T. and Hasegawa, S. (1988) *Eur. J. Pharmacol.* 154, 227–228.
- [6] Inoue, Y., Yanagisawa, M., Kimura, S., Kasuya, Y., Miyauchi, T., Goto, K. and Masaki, T. (1989) *Proc. Natl. Acad. Sci. USA* 86, 2863–2867.
- [7] Merrifield, R.B. (1963) *J. Am. Chem. Soc.* 85, 2149–2154.
- [8] Stewart, J.M. and Young, J.D. (1984) *Solid Phase Peptide Synthesis*, Pierce Chemical Co., Rockford, IL.
- [9] Tam, J.P., Heath, W.F. and Merrifield, R.B. (1983) *J. Am. Chem. Soc.* 105, 6442–6455.
- [10] Pelton, J.T., Kazmierski, W., Gulya, K., Yamamura, H.I. and Hruby, V.J. (1986) *J. Med. Chem.* 29, 2370–2375.
- [11] Wüthrich, K. (1986) *NMR of Proteins and Nucleic Acids*, John Wiley and Sons, New York.
- [12] Marion, E. and Wüthrich, K. (1983) *Biochem. Biophys. Res. Commun.* 113, 967–974.
- [13] Rance, M., Sorensen, O.W., Bodenhausen, G., Wagner, G., Ernst, R.R. and Wüthrich, K. (1983) *Biochem. Biophys. Res. Commun.* 117, 479–485.
- [14] Wagner, G. (1983) *J. Magn. Resonance* 55, 151–156.
- [15] Anil-Kumar, Ernst, R.R. and Wüthrich, K. (1980) *Biochem. Biophys. Res. Commun.* 95, 1–6; Rance, M., Sorensen, O.W., Bodenhausen, G., Wagner, G., Ernst, R.R. and Wüthrich, K. (1983) *Biochem. Biophys. Res. Commun.* 117, 479–485.
- [16] SYBYL Molecular Modeling Software, version 5.1, Tripos Associates, St. Louis, MO.
- [17] Singh, V.C., Weiner, P.K., Coldwell, J.W. and Kollman, P.A. (1986) *AMBER (UCSF version 3.0)*, Dept Pharmaceutical Chemistry, University of California, San Francisco.
- [18] Sugeta, H., Go and Miyazawa, T. (1973) *Bull. Chem. Soc. Jap.* 46, 3407–3411.